Published in final edited form as:
Pharm Res. 2009 June ; 26(6): 1407–1418. doi:10.1007/s11095-009-9851-0.

Targetable HPMA Copolymer–Aminohexylgeldanamycin Conjugates for Prostate Cancer Therapy

Mark P. Borgman[1,2], **Abhijit Ray**[4,6], **Rohit B. Kolhatkar**[1,2], **Edward A. Sausville**[2,3], **Angelika M. Burger**[2,3,7], and **Hamidreza Ghandehari**[4,5,6,8]

[1]Department of Pharmaceutical Sciences, University of Maryland, Baltimore, Maryland 21201, USA

[2]Center for Nanomedicine and Cellular Delivery, University of Maryland, Baltimore, Maryland 21201, USA

[3]Greenebaum Cancer Center, University of Maryland, Baltimore, Maryland 21201, USA

[4]Department of Pharmaceutics and Pharmaceutical Chemistry, University of Utah, 383 Colorow Road, Room 343, Salt Lake City, Utah 84108, USA

[5]Department of Bioengineering, University of Utah, Salt Lake City, Utah 84108, USA

[6]Center for Nanomedicine, Nano Institute of Utah, University of Utah, Salt Lake City, Utah 84108, USA

[7]Barbara Ann Karmanos Cancer Institute and Department of Pharmacology, Wayne State University, Detroit, Michigan 48201, USA

Abstract

Purpose—This study focuses on the synthesis and characterization of *N*-(2-hydroxypropyl)methacrylamide (HPMA) copolymer–cyclo-RGD (Arg-Gly-Asp) conjugates for delivery of geldanamycin to prostate tumors.

Materials and Methods—HPMA copolymers containing aminohexylgeldanamycin (AH-GDM) with and without the targeting peptide RGDfK were synthesized and characterized. Drug release from copolymers was evaluated using cathepsin B. Competitive binding of copolymer conjugates to $\alpha_v\beta_3$ integrin was evaluated in prostate cancer (PC-3) and endothelial (HUVEC) cell lines and *in vitro* growth inhibition was assessed. The maximum tolerated dose for single i.v. injections of free drug and the conjugates was established in nude mice.

Results—HPMA copolymers containing AH-GDM and RGDfK showed active binding to the $\alpha_v\beta_3$ integrin similar to that of free peptide. Similarly, growth inhibition of cells by conjugates was comparable to that of the free drug. Single intravenous doses of HPMA copolymer–AH-GDM–RGDfK conjugates in mice were tolerated at 80mg/kg drug equivalent, while free drug caused morbidity at 40mg/kg. No signs of toxicity were present in mice receiving HPMA copolymer-AH-GDM-RGDfK over the 14-day evaluation period.

Conclusion—Results of *in vitro* activity and *in vivo* tolerability experiments hold promise for the utility of HPMA copolymer–AH-GDM–RGDfK conjugates for treatment of prostate cancer with greater efficacy and reduced toxicity.

[8]To whom correspondence should be addressed. (hamid.ghandehari@pharm.utah.edu).

Keywords

geldanamycin; HPMA copolymer; prostate cancer; RGDfK; targeted delivery

INTRODUCTION

Prostate cancer is the second leading cause of cancer related deaths among men in the United States (1). Geldanamycin (GDM) is a benzoquinoid ansamycin (2) that has been extensively studied for its antitumoral efficacy (3). It binds with high affinity to the chaperone protein heat-shock protein 90 (HSP90), inhibiting its ability to fold client proteins into their active conformation. HSP90 clients include several proteins of potential importance in mediating prostate cancer progression, including wild-type and mutated androgen receptor, HER2 and Akt, and hence particular interest exists for treatment of prostate cancer with HSP90 inhibitors (4–6).

Clinical investigations with geldanamycin were thwarted due to hepatic toxicity (3) and analogs of GDM were synthesized that could provide equal or greater potency and reduced toxicity. One such analog, 17-allylamino-17-demethoxygeldanamycin (17-AAG) (7) is currently being evaluated in phase II clinical trials for its antitumor efficacy (4). Additionally, a water soluble derivative 17-dimethylaminoethylamino-17-demethoxygeldanamycin (17-DMAG) (8), with improved aqueous formulation properties and potential for oral absorption (9), is currently in phase I clinical trials (4). While progress has been made to reduce the toxicity of the parent drug, clinical response is still limited (10). Advancements in geldanamycin delivery to tumor sites where toxicity is reduced are necessary to fully realize the clinical potential of this drug (11).

N-(2-Hydroxypropyl)methacrylamide (HPMA) copolymers have been widely used as polymeric delivery systems to modify the biodistribution of toxic drugs (12). Previous investigations have identified HPMA copolymer–cyclo-RGD (Arg-Gly-Asp) conjugates that increase tumor accumulation compared to non-targeted systems (13–15). This accumulation takes place through specific interaction of RGD motifs present in the copolymer side chains with $\alpha_v\beta_3$ integrins over-expressed on angiogenic blood vessels (16) and some cancer cell types (17). These copolymers also benefit from passive tumor accumulation through the enhanced permeability and retention (EPR) effect (18) whereby macromolecules extravasate into tumor tissue through discontinuous blood vessels and are entrapped there due to poor lymphatic drainage. Enhanced accumulation was also demonstrated by active targeting in various human prostate cancer xenografts (19).

HPMA copolymers used as drug carriers are typically designed with the drug molecule attached to the copolymer backbone via the lysosomally degradable sequence Gly-Phe-Leu-Gly (20), as is the case in the present report. This sequence allows for specific intracellular release of drug by lysosomal proteases such as cathepsin B while remaining stable during *in vivo* trafficking to tumor sites (21). Previously, HPMA copolymer–geldanamycin conjugates have shown efficacy *in vitro* against human ovarian carcinoma cell lines (22, 23). To allow for geldanamycin conjugation to a monomeric unit and subsequent polymerization into HPMA copolymers, the parent GDM drug molecule must be derivatized at position 17 with a reactive amino group. The structure 17-(6-aminohexylamino)-17-demethoxygeldanamycin (AH-GDM) was attached to HPMA copolymers based on previous investigations demonstrating favorable stability and *in vitro* activity (23).

Geldanamycin derivatives are known to have antiangiogenic and antitumoral effects (9, 24–26). To improve targeting to endothelial and prostate cancer cells, in the present study we

have developed an HPMA copolymer–GDM–cyclo-RGD conjugate. The synthesis, characterization, *in vitro* growth inhibition of model prostate and endothelial cell lines and initial *in vivo* toxicity evaluation of these conjugates in nude mice are reported.

MATERIALS AND METHODS

Chemicals

Geldanamycin (NSC 122750) was kindly supplied by the National Cancer Institute Developmental Therapeutics Program (Dr. E. Tabibi) and the compound was protected from light during all procedures. RGDfK (MW 604.5) was obtained from AnaSpec Inc. (San Jose, CA) at >95% purity and used as supplied. *N*-(2-hydroxypropyl)methacrylamide (HPMA) (27); *N*-methacryloylglycylglycyl-*p*-nitrophenyl ester (MA-GG-ONp) (28); *N*-methacryloylglycylphenylalanylleucylglycine (MA-GFLG-OH) (29); *N*-methacryloylglycylphenylalanylleucylglycine-*p*-nitrophenyl ester (MA-GFLG-ONp) (29); and *N*-methacryloyl-tyrosinamide (MA-Tyr) (30) were synthesized and characterized according to previously described methods. Cathepsin B (CPB; 21.4 U/mg protein) and model substrate *N*-benzoyl-Phe-Val-Arg-*p*-nitroanilide hydrochloride were purchased from Sigma Chemical Co. (St. Louis, MO). Murine monoclonal anti-$\alpha_v\beta_3$ integrin antibody (LM609), murine IgG isotype control and FITC-conjugated goat antimouse IgG were obtained from Millipore (Billerica, MA). ^{125}I-echistatin (2,000 Ci/mmol) was purchased from Perkin Elmer (Waltham, MA). All amino acids used were of L-configuration. All other chemicals were of reagent grade as obtained from Sigma Chemical Co.

Synthesis and Characterization of GDM Derivatives and Comonomers

17-(6-Aminohexylamino)-17-demethoxygeldanamycin (AH-GDM) and *N*-methacryloylglycylphenylalanylleucylglycl-17-(6-aminohexylamino)-17-demethoxygeldanamycin (MA-GFLG-AH-GDM) were synthesized according to previously described procedures with minor modifications (22, 23, 31). Briefly, GDM (256 mg, 0.46 mmol) was dissolved in chloroform (30 ml) at 40°C, cooled to room temperature and added dropwise to a solution of 1,6-Diaminohexane (1.6 g, 13.8 mmol) in chloroform (120 ml). The reaction continued for 2 h with stirring. Deionized water was then added and the reaction mixture was washed numerous times with excess deionized water. Organic layer containing product was dried with anhydrous sodium sulfate and evaporated under vacuum. Product formation and purification was monitored by thin layer chromatography (TLC) (Rf=0.8 on silica gel, DCM/MeOH=7/3) and mass spectrometry (MS) (MW 645.2). MA-GFLG-AH-GDM was synthesized by adding AH-GDM (300 mg, 0.47 mmol) to a solution of MAGFLG- ONp (244 mg, 0.42 mmol) in anhydrous DMSO (75 ml) with stirring for 3 h. DMSO was removed under vacuum and pure product obtained by silica gel chromatography (EtOAc/MeOH=9/1). Product formation was monitored by MS (MW 1,109.5 (M^++23)) and collection was monitored by TLC (Rf=0.5 on silica gel, EtOAc/MeOH=9/1). Respective fractions were pooled, solvent removed and dried under vacuum. Structure of purified products AH-GDM and MA-GFLG-AH-GDM were confirmed by nuclear magnetic resonance (NMR) performed on a Varian INOVA 500 M Hz spectrometer using DMSO-d_6 as a solvent (data not shown) and compared with previously solved structures (23).

Water-soluble derivative AH-GDM hydrochloride (MW 645.2 (free base)) was synthesized by taking AH-GDM (232 mg, 0.36 mmol) dissolved in THF (6 ml) and adding dropwise 2.0 M HCl in diethyl ether (6 ml). AH-GDM hydrochloride precipitated immediately, solvent evaporated under vacuum, washed repeatedly with excess EtOAc, dried under vacuum, dissolved in water, filtered and lyophilized. Elemental analysis (Atlantic Microlab, Inc., Norcross, GA) calculated for AH-GDM·HCl·1.5H_2O ($C_{34}H_{53}N_4O_8Cl$·1.5 H_2O; C, 57.65; H, 7.96; N, 7.91; found: C, 57.60; H, 7.96; N, 7.77). Finally, to facilitate the HPLC analysis of

drug release products, the compound glycyl-AH-GDM (Gly-AH-GDM) was synthesized by reacting AH-GDM (10 mg, 15.5 μmol) with Fmoc-Gly-Cl (14.7 mg, 46.5 μmol) (32) for 3 h in anhydrous DCM in presence of Hunig's base (DIPEA). Fmoc-Gly-AH-GDM (MW 924.1) was used without any purification for next step to deprotect Fmoc using piperidine (1 ml in 4 ml DMF). The crude Gly-AH-GDM product obtained was purified by preparatory TLC (silica gel, DCM/ MeOH=9/1) (MW 701.9).

Synthesis and Characterization of HPMA Copolymer Conjugates

HPMA copolymers were synthesized via free radical precipitation copolymerization of comonomers in 10% *v*/*v* anhydrous dimethyl sulfoxide (DMSO) in acetone using *NN*′-azobisisobutyronitrile (AIBN) as the initiator (27). The feed composition of comonomers for all copolymers is given in Table I. The comonomer mixtures were sealed in an ampoule under nitrogen and stirred at 50°C for 24 h. Solvent was removed by rotary evaporation, copolymer precursor dissolved in methanol and precipitated and washed in diethyl ether. MA-GG-ONp content in the polymeric precursors was assessed by release of p-nitrophenol (ONp) from the copolymer in 1.0 N sodium hydroxide by UV spectrophotometry (400 nm). Weight average molecular weight (M_w) and poly-dispersity (M_w/M_n) were estimated by size exclusion chromatography (SEC) on a Superose 12 column (10mm×30 cm) (GE Healthcare, Piscataway, NJ) with fractions of known molecular weight HPMA copolymers using a Fast Protein Liquid Chromatography (FPLC) system (GE Healthcare).

HPMA copolymer–RGDfK conjugates (Table I, Fig. 1) were synthesized via *p*-nitrophenyl ester aminolysis of polymeric precursors in dry DMF in the presence of pyridine for 48 h (14). The reaction was terminated with 0.1 N sodium hydroxide. DMF was removed under vacuum. Copolymer precipitate was dissolved in deionized water and purified using Amicon Ultra-15 (MWCO 3000, Millipore) ultracentrifugal tubes to remove small molecular weight impurities. AH-GDM content was determined by UV spectrophotometric analysis of copolymer products not containing RGDfK using $\varepsilon^{340\ nm} = 2.16\times10^4\ M^{-1}\ cm^{-1}$ in DMSO and applied to copolymers containing RGDfK from the same precursor. The peptide content of the conjugates was determined by amino acid analysis (Commonwealth Biotechnologies, Richmond, VA).

Drug Release Studies

The *in vitro* release of AH-GDM from HPMA copolymers was evaluated using the model lysosomal enzyme cathepsin B (CPB) according to previously described procedures with minor modifications (23, 33, 34). Enzyme incubation mixture consisted of CPB stock solution (0.98 ml, 0.572 mg/ml (12.2 units/ml) in 0.1 M ammonium acetate buffer pH=5.5, 1 mM EDTA) and cysteine solution (0.02 ml, 250 mM in acetate buffer pH=5.5, 1 mM EDTA). 5 mg of HPMA copolymer–AH-GDM conjugates P1 and P2 (see Table I) were dissolved in the incubation mixture (1 ml, 5 min preincubation at 37°C). At 15, 60 and 180 min, 100 μl samples were removed, drug extracted twice with 1 ml ethyl acetate, organic layer separated and dried under nitrogen. Resulting residue was dissolved in 0.5 ml of mobile phase and evaluated for drug content using reverse-phase high performance liquid chromatography (HPLC). Mobile phase consisted of 0.05 M ammonium acetate buffer pH=4.7 and acetonitrile (65:35, *v*/*v*) at a flow rate of 1 ml/min (3). HPLC analyses were performed with a Waters 717 autosampler (Waters Corporation, Milford, MA) with Waters 2487 dual wavelength detector set at 350 nm using a Waters XBridge column (C18, 4.6×150 mm, 5 μm). The analytical column was protected with a Waters Xbridge guard column (C18, 4.6×20 mm, 5 μm). A calibration curve was generated by extracting and processing as noted above standard solutions of AH-GDM dissolved in 0.1 M ammonium acetate buffer pH=5.5 using the corresponding peak area *versus* concentration. Direct injections of standard solutions without extraction were used to determine extraction efficiency. Standard

solutions of Gly-AH-GDM were also used to identify release products. Percent drug release was calculated from the drug content of the copolymers measured by UV spectroscopy and the content of free drug quantified by HPLC. A stock solution of the standard substrate *N*-benzoyl-Phe-Val-Arg-*p*-nitroanilide hydrochloride (50 mM in DMSO) was used to verify enzyme activity at the given time intervals.

Cell Lines

The prostate cancer cell lines PC-3 and DU145 (ATCC, Manassas, VA) were cultured in RPMI 1640 media (Invitrogen, Carlsbad, CA) supplemented with 4mM L-glutamine, 10% (*v*/*v*) heat-inactivated fetal bovine serum (FBS) and 1% 100x antibiotic-antimycotic (Invitrogen) at 37°C in a humidified atmosphere of 5% CO_2 (*v*/*v*). HUVECs (35) were cultured in endothelial cell growth media-2 (EGM-2: Lonza, Walkersville, MD) at 37°C in a humidified atmosphere of 5% CO_2 (*v*/*v*). For all experimental procedures, sub-confluent cells in 24 h culture were harvested with 0.05% trypsin/0.02% EDTA in PBS.

Fluorescent-activated Cell Sorting (FACS)

The relative expression of the $\alpha_v\beta_3$ integrin on PC-3, DU145 and HUVEC cells was determined by fluorescence activated cell sorting using a modification of previously reported procedures (35). Cells were harvested, washed with PBS containing 10% fetal bovine serum, and resuspended in PBS containing 2% bovine serum albumin (BSA). Cells (5×10^5) in suspension were then incubated with 0.5 μg (in 5 μl buffer) mouse anti-$\alpha_v\beta_3$ integrin IgG or mouse IgG isotype control at room temperature for 1 h. Primary antibody was removed by three washes with PBS (2% BSA) and cell pellets resuspended with FITC-labeled goat anti-mouse IgG in the same buffer. Following incubation in dark for 30 min, cells were washed (3×) and resuspended in PBS (1 mL). Cell suspensions were analyzed using a Beckton Dickinson FACScan analyzer (Franklin Lakes, NJ). Each experiment was done in triplicate.

Cell Receptor Binding Assay

The binding affinities of free RGDfK peptide and HPMA copolymer conjugates were assessed using a competitive binding assay to $\alpha_v\beta_3$ integrin expressed on PC-3 and HUVEC cells with ^{125}I-echistatin (36–38). PC-3 and HUVEC cells were harvested, washed with PBS, resuspended in binding buffer (20 mmol/L Tris, pH 7.4, 150 mmol/L NaCl, 2 mmol/L $CaCl_2$1 mmol/L $MgCl_2$1 mmol/L $MnCl_2$0.1% BSA) and seeded in 96-well Multiscreen HV filter plates (0.45 μm; Millipore) at 50,000 cells per well. Cells were co-incubated at 4°C for 2 h with ^{125}I-echistatin (0.05 nM) and increasing peptide equivalent concentrations of copolymers or free RGDfK (0–500 μM), and final volume adjusted to 200 μL all in binding buffer. Following incubation, the plates were filtered using a Multiscreen vacuum manifold (Millipore) and washed twice with cold binding buffer. Filters were harvested and radioactivity determined by γ-counting (Perkin Elmer Wizard, 1470 Automatic Gamma Counter) to determine percent bound ^{125}I-echistatin. Nonspecific binding was determined by incubating cells with a 200-fold excess of cold echistatin. Nonlinear regression analysis and determination of IC_{50} values was performed using GraphPad Prism (GraphPad Software, Inc.).

In Vitro Growth Inhibition

Growth inhibition effect and GI_{50} dose of free drug and copolymers was evaluated on PC-3, DU145 and HUVEC cell lines using a modified MTT procedure (39). 7,500 PC-3, 4,000 DU145 or 8,000 HUVEC cells per well were seeded in 96-well microtiter plates and plated for 24 h. On day 0 cells were treated with drug and copolymer solutions in complete media lasting for 72 h. Following treatments, MTT solution (0.2 mg/ml final concentration) was

added for 4 h, media gently aspirated, formazan crystals dissolved in DMSO and absorption measured at 550 nm with blank well correction. Cell growth inhibition was determined by subtracting the cell viability at day 0 from the cell viability after 72 h treatment and expressed as % cell viability compared to untreated cells. Experiments were routinely conducted in the exponential growth phase. GI_{50} values were determined by nonlinear regression analysis using GraphPad Prism software.

Dose Range Finding and Toxicity Evaluation in Mice

Initial evaluation of tolerability and toxicity of AH-GDM and HPMA copolymer–AH-GDM–RGDfK conjugates (P1) was conducted in 7–8 week old female athymic NCr-*nu/nu* mice (Animal Production Facility at NCI Frederick, MD) according to previously described methods for HPMA copolymer conjugates (40). Mice were injected intravenously (i.v.) via the tail vein with sterile solutions of AH-GDM hydrochloride (20, 30 and 40 mg/kg) and P1 (40, 60 and 80 mg/kg drug equivalent) in saline. Control mice were injected with equal volumes of saline. Mice were monitored for 14 days post-injection for visual signs of toxicity, and body weight was recorded. On day 14, necropsies were performed to assess liver, kidney and spleen organ weights. Each organ was then fixed in 10% neutral buffered formalin, embedded in paraffin, cut and mounted in 5 μm sections, hematoxylin and eosin stained and histological evaluation for organ specific indicators of toxicity performed (Mass Histology Service, Worcester, MA). Blood was collected post mortem from the axillary vessels into heparinized tubes and analyzed with the Abaxis VetScan® Classic (Abaxis, Union City, CA) serum chemistry analyzer for hepatic and renal toxicity indicators. Three mice were treated per group except in the cases where acute morbidity was expected (e.g. free drug), then only two mice were evaluated in order to limit animal suffering and use. All studies were conducted under an approved protocol of the University of Maryland Baltimore Institutional Animal Care and Use Committee (IACUC).

Statistical Analysis

Differences in drug release, $\alpha_v\beta_3$ integrin expression, drug-free polymer cytotoxicity, mouse body weight and organ weight were analyzed using one-way ANOVA. Where differences were detected, Tukey's test was used to test for pairwise differences between the groups.

RESULTS

Characteristics of HPMA Copolymer Conjugates

Drug derivative AH-GDM and drug comonomer MAGFLG- AH-GDM were synthesized and characterized, and retained identical structural properties as previously reported (23). The characteristics of HPMA copolymers containing AH-GDM and RGDfK are summarized in Table I. Drug containing copolymers with (P1) and without (P2) RGDfK peptide targeting moiety were synthesized with an estimated molecular weight of 25.0 kDa and polydispersity 1.6 (for precursor) with 10.8% (*w*/*w*) drug content. Copolymers were also synthesized containing the degradable peptide sequence Gly-Phe-Leu-Gly without drug attached (P3, P4) with estimated molecular weight of 47.0 kDa (for precursor), and additionally conjugated with RGDfK (P3). RGDfK content in conjugates P1, P3, and P5 were relatively similar with 0.242, 0.233 and 0.165 mmol peptide per gram polymer, respectively.

Cathepsin B Catalyzed Drug Release from HPMA Copolymer–AH-GDM Conjugates

Extent of drug release from HPMA copolymer products was evaluated at 15, 60 and 180 min (Table II). Predominant drug release products resulting from CPB catalyzed release were identified and quantified by RP-HPLC. Extraction efficiency was calculated to be

96%. Incubation with CPB resulted in the generation of AH-GDM and Gly-AH-GDM release products. Total drug release from P2 (no RGDfK in backbone) was significantly ($p<0.001$) greater than drug release for P1 at all time points. The difference in drug release between the two copolymers was also significant ($p<0.001$) for AHGDM and Gly-AH-GDM products. Additionally, for each copolymer at each time point, Gly-AH-GDM release was significantly ($p<0.001$) greater than the release of AH-GDM.

Expression of $\alpha_v\beta_3$ Integrin and Competitive Binding

All cell lines tested expressed the $\alpha_v\beta_3$ integrin as detected by immunofluorescence staining and fluorescence activated cell sorting (Fig. 2). Highest levels of the integrins were observed for HUVECs with 76.2±1.4% of cells expressing the receptor as compared to isotype control. This is a significantly ($p<0.001$) higher expression as compared to DU145 (46.1±1.7% of cells as compared to isotype control) and PC-3 (38.5±3.3% of cells as compared to isotype control) cell lines. Additionally, DU145 cells had significantly ($p< 0.05$) higher expression as compared to PC-3.

Competitive binding studies with HUVEC and PC-3 cells showed active binding of RGDfK peptide and copolymer– peptide conjugate (P1) to the $\alpha_v\beta_3$ integrin (Fig. 3). IC_{50} values (nM peptide) as determined by non-linear regression for binding to PC-3 cells were 2,033±1.09 and 3,971±1.24 for RGDfK and P1, respectively. IC_{50} values (nM peptide) for binding to HUVECs were 334.5±1.14 and 594.6±1.22 for RGDfK and P1, respectively. At equivalent peptide concentration, free RGDfK peptide shows greater displacement and binding affinity as compared to polymeric conjugates. Copolymers without RGDfK peptide did not show active binding.

In Vitro Growth Inhibition

Antiproliferative activity of drug and copolymer–drug conjugates in PC-3, DU145 and HUVEC cells are shown in Fig. 4. GI_{50} values for all treatments were determined by nonlinear regression and are given in Table III. Results for GDM and AH-GDM drug treatments show that substitution of GDM at position 17 decreases its efficacy and is consistent with previous reports (22). However, attachment of AHGDM to HPMA copolymer–RGDfK conjugates does not greatly affect GI_{50}. P1 copolymer with drug and peptide attached demonstrated greater efficacy as measured by GI_{50} compared to non-targeted copolymer P2.

PC-3, DU145 and HUVEC cells were additionally treated with drug-free control polymers P3-P5 at equivalent polymer concentrations corresponding to those used for drug-containing copolymer experiments (Fig. 5). Growth inhibition studies showed an effect on cell viability at high concentrations of the copolymers. No significant change in cell viability was observed for drug- and peptide-free copolymer P4 except in the case of HUVEC cells (at high concentration) as compared to untreated cells. The presence of RGDfK on the copolymer backbone for P3 and P5 had a moderate effect on cell viability, and more so for HUVEC cells. However, drug-containing copolymers P1 and P2 had consistently greater toxic effect compared to drugfree copolymers at 1.2 mg/ml equivalent polymer concentration for all cell lines ($p<0.001$).

Tolerability and Toxicity of HPMA Copolymer–AH-GDM–RGDfK Conjugates

Initial tolerability and toxicity studies of single i.v. doses of AH-GDM hydrochloride and HPMA copolymer–AHGDM–RGDfK conjugate (P1) was assessed in nude mice (Table IV). The maximum tolerated dose of AH-GDM in this study was shown to be 30 mg/kg. At 40 mg/kg AH-GDM, mice showed signs of acute toxicity and became moribund in less than 1 min, necessitating euthanasia. In contrast, doses of P1 were tolerated at 80 mg/kg drug

equivalent. Further dose increases for P1 were not studied due to limitations in viscosity of polymer formulation for mouse i.v. administration. Toxicity in mice following treatment was monitored by body weight loss for 14 days (Fig. 6a). No decrease in body weight was observed for any treatments as compared to control. Additionally, liver, kidney and spleen organ weights were measured on day 14 following necropsy (Fig. 6b) and showed no significant difference compared to control mice.

Serum chemistry analysis was performed to further assess possible toxic effects of intravenously administered AH-GDM and P1 in mice compared to vehicle and untreated control animals. Data for select serum chemistry parameters indicative of liver or kidney toxicity when elevated are reported in Table V. Overall, the serum data indicates no signs of toxicity on day 14 with all values within the normal range of control mice. Additionally, histological analysis of liver, kidney and spleen sections showed healthy tissue and revealed no signs of toxicity or tissue damage (data not shown).

DISCUSSION

This study has evaluated the synthesis, characterization, *in vitro* binding and growth inhibition, and *in vivo* tolerability and toxicity of a new HPMA copolymer–RGDfK–amino-hexylgeldanamycin conjugate. Research from our laboratory has previously described HPMA copolymer–RGD peptide conjugates with enhanced accumulation in solid tumors (13, 14). This is the first report of using HPMA copolymer– RGD conjugates for delivery of chemotherapeutic agents. Previously studied was the anti-cancer effect of delivery of therapeutic radionuclides with a similar polymer platform (15). These copolymer conjugates can be used to actively deliver therapeutic agents to a broad spectrum of angiogenic tumors. This work has focused on the targeted delivery of geldanamycin to prostate cancer in order to maximize local delivery of the agent while altering biodistribution to reduce dose-limiting toxicity. HSP90 inhibitors such as geldanamycin are promising therapies for treatment of prostate cancer (4). Two derivatives of geldanamycin, 17-AAG and 17-DMAG, are currently in phase I and II clinical investigations for treatment of urologic malignancies, however dose-limiting toxicities remain an issue (4, 7, 10, 41, 42).

HPMA copolymers were successfully synthesized and characterized containing RGDfK and AH-GDM. Derivatizing geldanamycin is necessary to create a reactive molecule capable of polymer incorporation. The geldanamycin derivative AH-GDM was used in this study because of its favorable stability in PBS at 37°C and greater *in vitro* efficacy in the polymer-bound state as compared to other amino-alkyl geldanamycin derivatives (23). The monocyclic RGDfK was chosen for targeting to $\alpha_v\beta_3$ integrins. This peptide has a higher affinity than linear RGD sequences and greater solution stability than other doubly cyclized or linear peptide versions (43–45). The RGDfK peptide ligand actively targets the $\alpha_v\beta_3$ integrin and can enhance the cellular entry of HPMA copolymer conjugates through receptor-mediated internalization of conjugates bound to the $\alpha_v\beta_3$ integrin (46). This should result in drug release from the copolymers that occurs via enzymatic degradation of GFLG peptide sequences in the lysosomal compartment.

Drug release from the conjugates was evaluated *in vitro* with the model lysosomal enzyme CPB to understand the extent of, and differences in, release profiles of copolymers with and without RGDfK. RP-HPLC was employed to accurately identify and quantify the release products of the drug delivery system. The experimental time frame was limited to 3 h because further incubation in acetate buffer (pH=5.5) at 37°C resulted in degradation of released products (data not shown). In the absence of the RGDfK targeting moiety, enzymatically catalyzed drug release was enhanced (see Table II). This may be due to the limited accessibility of degradable peptide sequences to the active site of CPB when HPMA

copolymer backbones contain the bulky RGDfK. Initial drug release studies were used to optimize detection of release products using RP-HPLC following method development for AH-GDM standards. Results of these studies revealed that CPB-catalyzed drug release was generating native AH-GDM and a second unknown release product. Mass spectroscopic analysis of release mixtures, chemical synthesis of Gly-AH-GDM and HPLC analysis of standard compounds confirmed the second release product as Gly-AH-GDM.

Prior to *in vitro* testing, establishing the presence and relative expression of the $\alpha_v\beta_3$ integrin on our PC-3, DU145 and HUVEC cell lines was necessary to correlate with binding and growth inhibition studies. This was accomplished through incubation with an $\alpha_v\beta_3$ integrin-specific antibody and subsequent secondary fluorescent antibody staining and FACS. Results were as predicted with the highest integrin expression on HUVEC cells (See Fig. 2). It can be assumed that the endothelial nature of these cells explains the higher presence of integrin necessary for attachment to basement membranes and cellular migration during angiogenesis (16). Also encouraging to find was the presence of the integrin on the prostate cancer cell lines, necessary for tumor cell invasion and migration (17). Competitive binding results showed active binding of RGDfK and P1 conjugate (See Fig. 3), with RGDfK binding affinity on HUVECs similar to what has previously been shown (38). Most importantly, these studies showed that the affinity of copolymer conjugates is similar to that of free peptide, even when incubated at equivalent concentration of peptide. Additionally, incubation with drug containing copolymer P2 had no effect on radio-ligand displacement. Previous studies (19) by our laboratory have confirmed that control RGD peptide (namely RGE4C) does not bind to the integrin on HUVEC cells and thus its use has not been incorporated into the current studies.

Consistent with previous reports, cytotoxic effect of GDM is diminished when derivatized to an amino-alkyl form (in our case AH-GDM) (22). Growth inhibition results showed that HPMA copolymer–AH-GDM–RGDfK conjugates affected cell proliferation comparable with that of free drug (see Table III). This is despite previous reports that a decrease in activity of the free drug was observed upon copolymer incorporation (22, 23). This difference may be due to the presence of the RGDfK on the copolymer side chains either: (1) causing an increased amount of intracellular accumulation of the conjugates due to receptor mediated uptake, or (2) a toxic effect on cells from the RGDfK itself. The experiments presented here cannot fully explain this effect, however HPMA copolymers bearing only RGDfK show growth inhibition properties (see Fig. 5). It has been shown previously that RGD peptides alone can induce apoptosis in breast cancer cell lines (47), and that sensitivity of tumor cells to chemotherapeutics may be enhanced by concomitant administration with RGD peptides (48). This may explain our observed phenomena of *in vitro* cytotoxicity from HPMA copolymer–RGDfK conjugates. Most importantly when considering the case for *in vivo* efficacy, the possible effect of RGDfK on the side chains causing growth inhibition can be beneficial in the treatment of solid tumors.

Growth inhibition results show lower susceptibility of HUVEC cells compared to prostate cell lines for drug-containing copolymer P1 (Fig. 4 and Table III) whereas greater effect is observed on HUVEC cells with HPMA copolymer–RGDfK conjugates not containing drug as compared to PC-3 and DU145 (Fig. 5). This indicates that HUVECs may be less susceptible to AH-GDM delivered on HPMA copolymers as the prostate cancer cells, especially when considering HUVECs demonstrated the highest amount of $\alpha_v\beta_3$ integrin expression.

It is well known that the following three critical steps are required for cytotoxic activity of targeted polymer–drug conjugates: (1) cellular recognition of the polymer, (2) release of free drug from the polymer and (3) sensitivity of the cell toward the drug. The relative

contribution of each of these factors towards *in vitro* cytotoxicity is not clear. The current study demonstrates that sensitivity of the therapeutic agent (AH-GDM) towards cancer cell lines overrides targeting efficiency of the HPMA copolymers. For all cell lines studied a consistent decrease in IC_{50} values for targeted conjugates compared to non-targeted systems demonstrates the importance of the targeting peptide. However no correlation was observed for cytotoxicity and $\alpha_v\beta_3$ receptor expression or binding affinity of targeted copolymer for different cell lines. Thus, P1 showed much more cytotoxicity towards PC-3 in spite of showing higher binding affinity towards HUVECs. These results can be explained based on the variation in sensitivity of different cell lines towards AH-GDM. The rank order for sensitivity of cancer cell lines towards AH-GDM was found to be DU145>PC-3>HUVEC. This rank order was retained in targeted delivery systems, thus P1 showing 1.77 and 14-fold more cytotoxicity towards DU145 compared to PC-3 and HUVECs respectively. Overall these studies demonstrate that the presence of receptors on cell surface is important, but level of receptor expression has much less contribution towards cytotoxicity. Drug release from copolymers follows internalization and higher quantities of released drug in tumor should impart the best efficacy. In spite of lower drug release, targeted HPMA copolymer (P1) showed higher cytotoxicity compared to its non-targeted counterpart (P2). Other investigators (49, 50) have also found a lack of correlation between drug release and cytotoxicity and suggested that although intracellular drug release is important, it is not the only factor affecting cytotoxicity. Both conjugates evaluated in the current study showed modest amount of drug release within a short period of time.

The hydrochloride salt version of AH-GDM was synthesized for its water-solubility and used for *in vivo* studies to accurately compare tolerated doses following i.v. injection. This proved to be beneficial because both parent drug AHGDM and copolymer–drug conjugate P1 were readily soluble in saline for parenteral administration. A dose of 40 mg/kg AH-GDM caused acute toxicity while mice treated with 30 mg/ kg AH-GDM survived. This indicates the maximum tolerated dose (MTD) lies within that range, and is similar to the previously reported MTD for intravenously administered GDM (3). On the other hand, P1 was administered successfully at 80 mg/kg with no signs of toxicity. That dose reaches the upper limit of achievable formulation in saline before the solution becomes too viscous. Thus, in the case for copolymer administration the maximum dose is not limited by tolerance rather by formulation properties. Despite the acute toxicity seen in the highest dose of free drug, no longer-term toxicity was observed for remaining groups. Body weight and organ weights were all increased or not significantly different than untreated controls (Fig. 6). This was further confirmed by histology examination of liver, kidney and spleen organ sections showing healthy tissue. Serum chemistry analysis was also used to detect liver damage by increased levels of alanine aminotransferase, alkaline phosphatase, total bilirubin, or decreased albumin and total protein (51). Additionally, renal function was evaluated via blood urea nitrogen levels that would be increased if kidney function was impaired (51). All results showed normal levels of these analytes. Overall, the tolerance of HPMA copolymer– AH-GDM–RGDfK conjugates *in vivo* and the *in vitro* activity of the conjugates against prostate cancer cell lines offer significant advantages for targeted delivery of geldanamycin to solid tumors with a high therapeutic window. The high polymer-drug doses that can be administered in mice and the anticipation based on prior experience of increased accumulation of the delivery system at the tumor site (13) suggest that efficacious drug concentrations can be achieved. Thus, further preclinical tumor uptake and efficacy studies are warranted.

CONCLUSIONS

HPMA copolymer–AH-GDM–RGDfK conjugates showed growth inhibition activity *in vitro* against prostate and endothelial cell lines. Active binding to the $\alpha_v\beta_3$ integrin was

demonstrated suggesting that these conjugates have the ability to target solid prostate tumors *in vivo*. *In vitro* results, along with favorable tolerability of these conjugates *in vivo* compared to free drug make them a promising drug delivery strategy to improve water solubility, reduce toxicity and increase efficacy of geldanamycins.

Acknowledgments

This research was supported by National Institutes of Health grant R01 EB007171. RK is supported by Department of Defense Multidisciplinary Postdoctoral Fellowship W81XWH-06-1-0698. MB is supported in part by the American Foundation for Pharmaceutical Education and University of Maryland Department of Pharmaceutical Sciences predoctoral fellowships.

ABBREVIATIONS

17-AAG	17-allylamino-17-demethoxygel danamycin
17-DMAG	17-dimethylaminoethylamino-17-deme thoxygeldanamycin
AH	6-aminohexylamino
AH-GDM	17-(6-aminohexylamino)-17-demethoxygeldanamycin
CPB	cathepsin B
DCM	dichloromethane
DMSO	dimethyl sulfoxide
EtOAc	ethyl acetate
GDM	geldanamycin (GDM)
HPLC	high performance liquid chromatography
HPMA	*N*-(2-hydroxypropyl) metha crylamide
MA-GFLG-AH-GDM	*N*-methacryloylglycylphenylalanylleucylglycl-17-(6-aminohexylamino)-17-demethoxygeldanamycin
MeOH	methanol
RGDfK	cyclo-(arginine-glycince- aspartic acid-D-phenylalanine-lysine)
THF	tetrahydrofuran

REFERENCES

1. American Cancer Society. Cancer Facts & Figures 2008. Atlanta: American Cancer Society; 2008.
2. DeBoer C, Meulman PA, Wnuk RJ, Peterson DH. Geldanamycin, a new antibiotic. J. Antibiot. (Tokyo). 1970; 23:442–447. [PubMed: 5459626]
3. Supko JG, Hickman RL, Grever MR, Malspeis L. Preclinical pharmacologic evaluation of geldanamycin as an antitumor agent. Cancer Chemother. Pharmacol. 1995; 36:305–315. [PubMed: 7628050]
4. Lattouf JB, Srinivasan R, Pinto PA, Linehan WM, Neckers L. Mechanisms of disease: the role of heat-shock protein 90 in genitourinary malignancy. Nat. Clin. Pract. Urol. 2006; 3:590–601. [PubMed: 17088927]
5. Rocchi P, So A, Kojima S, Signaevsky M, Beraldi E, Fazli L, Hurtado-Coll A, Yamanaka K, Gleave M. Heat shock protein 27 increases after androgen ablation and plays a cytoprotective role in hormone-refractory prostate cancer. Cancer Res. 2004; 64:6595–6602. [PubMed: 15374973]
6. Solit DB, Scher HI, Rosen N. Hsp90 as a therapeutic target in prostate cancer. Semin. Oncol. 2003; 30:709–716. [PubMed: 14571418]

7. Schnur RC, Corman ML, Gallaschun RJ, Cooper BA, Dee MF, Doty JL, Muzzi ML, Moyer JD, DiOrio CI, Barbacci EG, et al. Inhibition of the oncogene product p185erb B-2 *in vitro* and *in vivo* by geldanamycin and dihydrogeldanamycin derivatives. J. Med. Chem. 1995; 38:3806–3812. [PubMed: 7562911]
8. Egorin MJ, Lagattuta TF, Hamburger DR, Covey JM, White KD, Musser SM, Eiseman JL. Pharmacokinetics, tissue distribution, and metabolism of 17-(dimethylaminoethylamino)-17-demethoxygeldanamycin (NSC 707545) in CD2F1 mice and Fischer 344 rats. Cancer Chemother. Pharmacol. 2002; 49:7–19. [PubMed: 11855755]
9. Hollingshead M, Alley M, Burger AM, Borgel S, Pacula-Cox C, Fiebig HH, Sausville EA. *In vivo* antitumor efficacy of 17-DMAG (17-dimethylaminoethylamino-17-demethoxygeldanamycin hydrochloride), a water-soluble geldanamycin derivative. Cancer Chemother. Pharmacol. 2005; 56:115–125. [PubMed: 15791458]
10. Banerji U, O'Donnell A, Scurr M, Pacey S, Stapleton S, Asad Y, Simmons L, Maloney A, Raynaud F, Campbell M, Walton M, Lakhani S, Kaye S, Workman P, Judson I. Phase I pharmacokinetic and pharmacodynamic study of 17-allylamino, 17-demethoxygeldanamycin in patients with advanced malignancies. J. Clin. Oncol. 2005; 23:4152–4161. [PubMed: 15961763]
11. Ronnen EA, Kondagunta GV, Ishill N, Sweeney SM, Deluca JK, Schwartz L, Bacik J, Motzer RJ. A phase II trial of 17-(Allylamino)-17-demethoxygeldanamycin in patients with papillary and clear cell renal cell carcinoma. Invest. New Drugs. 2006; 24:543–546. [PubMed: 16832603]
12. Kopecek J, Kopeckova P, Minko T, Lu Z. HPMA copolymer-anticancer drug conjugates: design, activity, and mechanism of action. Eur. J. Pharm. Biopharm. 2000; 50:61–81. [PubMed: 10840193]
13. Mitra A, Coleman T, Borgman M, Nan A, Ghandehari H, Line BR. Polymeric conjugates of mono- and bi-cyclic alphaVbeta3 binding peptides for tumor targeting. J. Control Release. 2006; 114:175–183. [PubMed: 16889865]
14. Mitra A, Mulholland J, Nan A, McNeill E, Ghandehari H, Line BR. Targeting tumor angiogenic vasculature using polymer-RGD conjugates. J. Control Release. 2005; 102:191–201. [PubMed: 15653145]
15. Mitra A, Nan A, Papadimitriou JC, Ghandehari H, Line BR. Polymer–peptide conjugates for angiogenesis targeted tumor radiotherapy. Nucl. Med. Biol. 2006; 33:43–52. [PubMed: 16459258]
16. Brooks PC, Clark RA, Cheresh DA. Requirement of vascular integrin alpha v beta 3 for angiogenesis. Science. 1994; 264:569–571. [PubMed: 7512751]
17. Hood JD, Cheresh DA. Role of integrins in cell invasion and migration. Nat. Rev. Cancer. 2002; 2:91–100. [PubMed: 12635172]
18. Maeda H, Wu J, Sawa T, Matsumura Y, Hori K. Tumor vascular permeability and the EPR effect in macromolecular therapeutics: a review. J. Control Release. 2000; 65:271–284. [PubMed: 10699287]
19. Line BR, Mitra A, Nan A, Ghandehari H. Targeting tumor angiogenesis: comparison of peptide and polymer-peptide conjugates. J. Nucl. Med. 2005; 46:1552–1560. [PubMed: 16157540]
20. Rejmanova P, Kopecek J, Pohl J, Baudys M, Kostka V. Polymers containing enzymatically degradable bonds, 8. Degradation of oligopeptide sequences in N-(2-hydroxypropyl) methacrylamide copolymers by bovine spleen cathepsin B. Makromol. Chem. 1983; 184:2009–2020.
21. Putnam D, Kopeček J. Polymer conjugates with anticancer activity. Biopolymers. 1995; II:55–123.
22. Kasuya Y, Lu ZR, Kopeckova P, Minko T, Tabibi SE, Kopecek J. Synthesis and characterization of HPMA copolymer-aminopropylgeldanamycin conjugates. J. Control Release. 2001; 74:203–211. [PubMed: 11489496]
23. Kasuya Y, Lu ZR, Kopecková P, Tabibi SE, Kopecek J. Influence of the structure of drug moieties on the *in vitro* efficacy of HPMA copolymer–geldanamycin derivative conjugates. Pharm. Res. 2002; 19:115–123. [PubMed: 11883637]
24. Kaur G, Belotti D, Burger AM, Fisher-Nielson K, Borsotti P, Riccardi E, Thillainathan J, Hollingshead M, Sausville EA, Giavazzi R. Antiangiogenic properties of 17-(dimethylaminoethylamino)-17-demethoxygeldanamycin: an orally bioavailable heat shock protein 90 modulator. Clin. Cancer Res. 2004; 10:4813–4821. [PubMed: 15269157]

25. Smith V, Sausville EA, Camalier RF, Fiebig HH, Burger AM. Comparison of 17-dimethylaminoethylamino-17-demethoxy-geldanamycin (17DMAG) and 17-allylamino-17-demethoxygeldanamycin (17AAG) *in vitro*: effects on Hsp90 and client proteins in melanoma models. Cancer Chemother. Pharmacol. 2005; 56:126–137. [PubMed: 15841378]
26. Burger AM, Fiebig HH, Stinson SF, Sausville EA. 17-(Allylamino)-17-demethoxygeldanamycin activity in human melanoma models. Anti-Cancer Drugs. 2004; 15:377–387. [PubMed: 15057143]
27. Strohalm J, Kopecek J. Poly N-(2-hydroxypropyl) methacrylamide: 4. Heterogenous polymerization. Angew. Makromol. Chem. 1978; 70:109–118.
28. Rejmanova P, Labsky J, Kopecek J. Aminolyses of monomeric and polymeric p-nitrophenyl esters of methacryloylated amino acids. Makromol. Chem. 1977; 178:2159–2168.
29. Ulbrich K, Subr V, Strohalm J, Plocova D, Jelinkova M, Rihova B. Polymeric drugs based on conjugates of synthetic and natural macromolecules. I. Synthesis and physico-chemical characterisation. J. Control Release. 2000; 64:63–79. [PubMed: 10640646]
30. Lee JH, Kopeckova P, Kopecek J, Andrade JD. Surface properties of copolymers of alkyl methacrylates with methoxy (polyethylene oxide) methacrylates and their application as protein-resistant coatings. Biomaterials. 1990; 11:455–464. [PubMed: 2242394]
31. Kasuya Y, Lu ZR, Kopecková P, Kopecek J. Improved synthesis and evaluation of 17-substituted aminoalkylgeldanamycin derivatives applicable to drug delivery systems. Bioorg. Med. Chem. Lett. 2001; 11:2089–2091. [PubMed: 11514145]
32. Carpino LA, Cohen BJ, Stephens KE, Sadat-Aalaee SY, Tien JH, Langridge DC. (Fluoren-9-ylmethoxy)carbonyl (Fmoc) amino acid chlorides. Synthesis, characterization, and application to the rapid synthesis of short peptide segments. J. Org. Chem. 1986; 51:3732–3734.
33. Wang D, Kopeckova JP, Minko T, Nanayakkara V, Kopecek J. Synthesis of starlike N-(2-hydroxypropyl)methacrylamide copolymers: potential drug carriers. Biomacromolecules. 2000; 1:313–319. [PubMed: 11710118]
34. Pan H, Kopeckova P, Wang D, Yang J, Miller S, Kopecek J. Water-soluble HPMA copolymer-prostaglandin E1 conjugates containing a cathepsin K sensitive spacer. J. Drug Target. 2006; 14:425–435. [PubMed: 17092842]
35. Rhim JS, Tsai WP, Chen ZQ, Chen Z, Van Waes C, Burger AM, Lautenberger JA. A human vascular endothelial cell model to study angiogenesis and tumorigenesis. Carcinogenesis. 1998; 19:673–681. [PubMed: 9600354]
36. Wu Y, Zhang X, Xiong Z, Cheng Z, Fisher DR, Liu S, Gambhir SS, Chen X. microPET imaging of glioma integrin {alpha}v{beta}3 expression using (64)Cu-labeled tetrameric RGD peptide. J. Nucl. Med. 2005; 46:1707–1718. [PubMed: 16204722]
37. Kumar CC, Nie H, Rogers CP, Malkowski M, Maxwell E, Catino JJ, Armstrong L. Biochemical characterization of the binding of echistatin to integrin alphavbeta3 receptor. J. Pharmacol. Exp. Ther. 1997; 283:843–853. [PubMed: 9353406]
38. Borgman MP, Coleman T, Kolhatkar RB, Geyser-Stoops S, Line BR, Ghandehari H. Tumor-targeted HPMA copolymer-(RGDfK)-(CHX-A″-DTPA) conjugates show in-creased kidney accumulation. J. Control Release. 2008; 132:193–199. [PubMed: 18687371]
39. Hayon T, Dvilansky A, Shpilberg O, Nathan I. Appraisal of the MTT-based assay as a useful tool for predicting drug chemosensitivity in leukemia. Leuk. Lymphoma. 2003; 44:1957–1962. [PubMed: 14738150]
40. Duncan R, Coatsworth JK, Burtles S. Preclinical toxicology of a novel polymeric antitumour agent: HPMA copolymer-doxorubicin (PK1). Hum. Exp. Toxicol. 1998; 17:93–104. [PubMed: 9506260]
41. Goetz MP, Toft D, Reid J, Ames M, Stensgard B, Safgren S, Adjei AA, Sloan J, Atherton P, Vasile V, Salazaar S, Adjei A, Croghan G, Erlichman C. Phase I trial of 17-allylamino-17-demethoxygeldanamycin in patients with advanced cancer. J. Clin. Oncol. 2005; 23:1078–87. [PubMed: 15718306]
42. Ramanathan RK, Egorin MJ, Eiseman JL, Ramalingam S, Friedland D, Agarwala SS, Ivy SP, Potter DM, Chatta G, Zuhowski EG, Stoller RG, Naret C, Guo J, Belani CP. Phase I and pharmacodynamic study of 17-(allylamino)-17-demethoxygeldanamycin in adult patients with refractory advanced cancers. Clin. Cancer Res. 2007; 13:1769–1774. [PubMed: 17363531]

43. Assa-Munt N, Jia X, Laakkonen P, Ruoslahti E. Solution structures and integrin binding activities of an RGD peptide with two isomers. Biochemistry. 2001; 40:2373–2378. [PubMed: 11327857]
44. Bogdanowich-Knipp SJ, Chakrabarti S, Williams TD, Dillman RK, Siahaan TJ. Solution stability of linear vs. cyclic RGD peptides. J. Pept. Res. 1999; 53:530–541. [PubMed: 10424348]
45. Koivunen E, Wang B, Ruoslahti E. Phage libraries displaying cyclic peptides with different ring sizes: ligand specificities of the RGD-directed integrins. Biotechnology (N Y). 1995; 13:265–270. [PubMed: 9634769]
46. Schraa AJ, Kok RJ, Berendsen AD, Moorlag HE, Bos EJ, Meijer DK, de Leij LF, Molema G. Endothelial cells internalize and degrade RGD-modified proteins developed for tumor vasculature targeting. J. Control Release. 2002; 83:241–251. [PubMed: 12363450]
47. Buckley CD, Pilling D, Henriquez NV, Parsonage G, Threlfall K, Scheel-Toellner D, Simmons DL, Akbar AN, Lord JM, Salmon M. RGD peptides induce apoptosis by direct caspase-3 activation. Nature. 1999; 397:534–539. [PubMed: 10028971]
48. Broxterman HJ, Hoekman K. Direct activation of caspases by RGD-peptides may increase drug sensitivity of tumour cells. Drug Resist. Updat. 1999; 2:139–141. [PubMed: 11504483]
49. Etrych T, Chytil P, Jelinkova M, Rihova B, Ulbrich K. Synthesis of HPMA copolymers containing doxorubicin bound via a hydrazone linkage. Effect of spacer on drug release and *in vitro* cytotoxicity. Macromol. Biosci. 2002; 2:43–52.
50. Jelinkova M, Strohalm J, Plocova D, Subr V, St'astny M, Ulbrich K, Rihova B. Targeting of human and mouse T-lymphocytes by monoclonal antibody-HPMA copolymer-doxorubicin conjugates directed against different T-cell surface antigens. J. Control Release. 1998; 52:253–270. [PubMed: 9743446]
51. Loeb, WF.; Quimby, FW. The Clinical Chemistry of Laboratory Animals. Ann Arbor: Edwards Brothers; 1999.

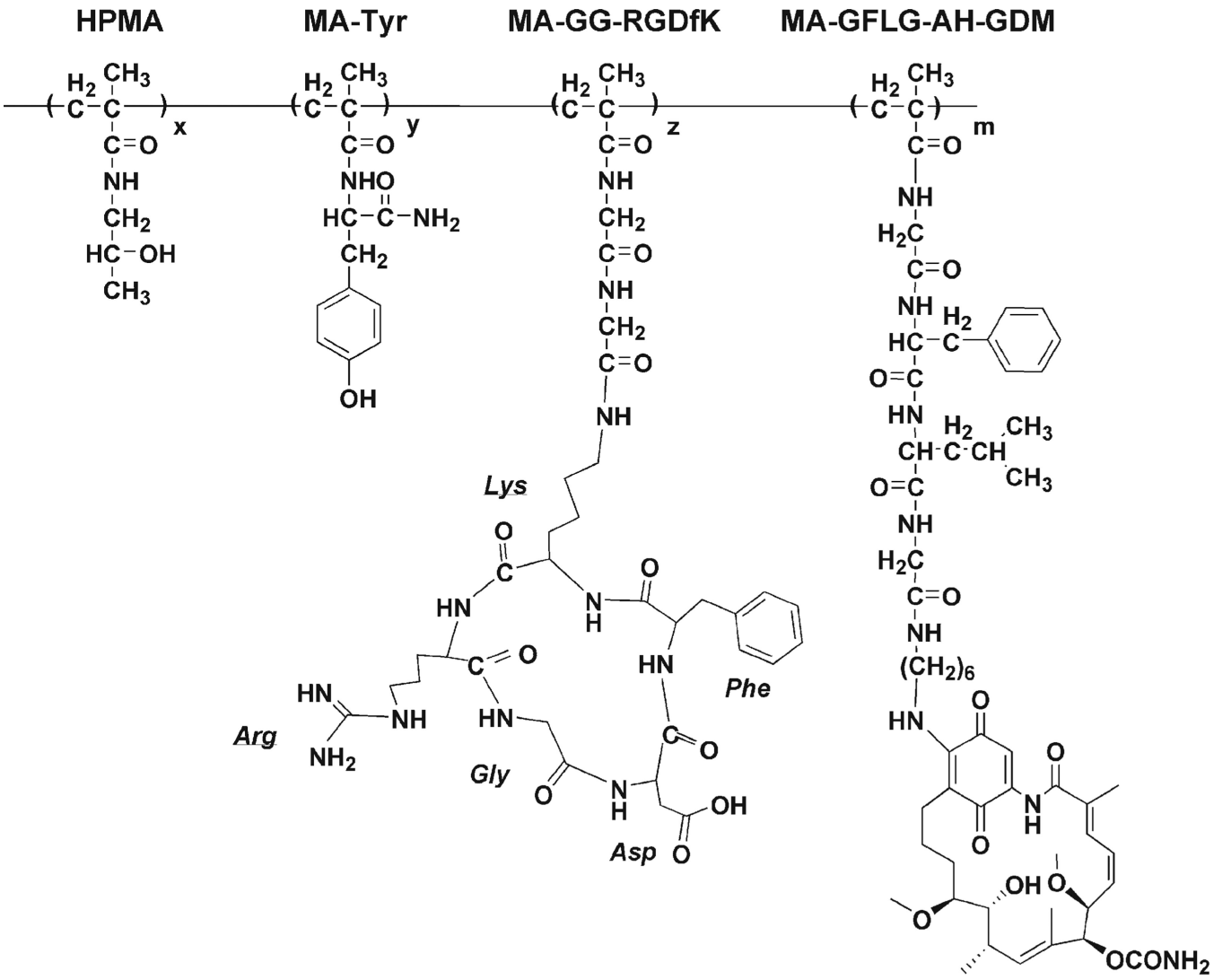

Fig. 1.

Structure of HPMA copolymer–RGDfK–AH-GDM (P1) conjugates. Select copolymers contained the monocyclized RGDfK peptide targeting moiety to target the geldanamycin derivative AH-GDM to the $\alpha_v\beta_3$ integrin.

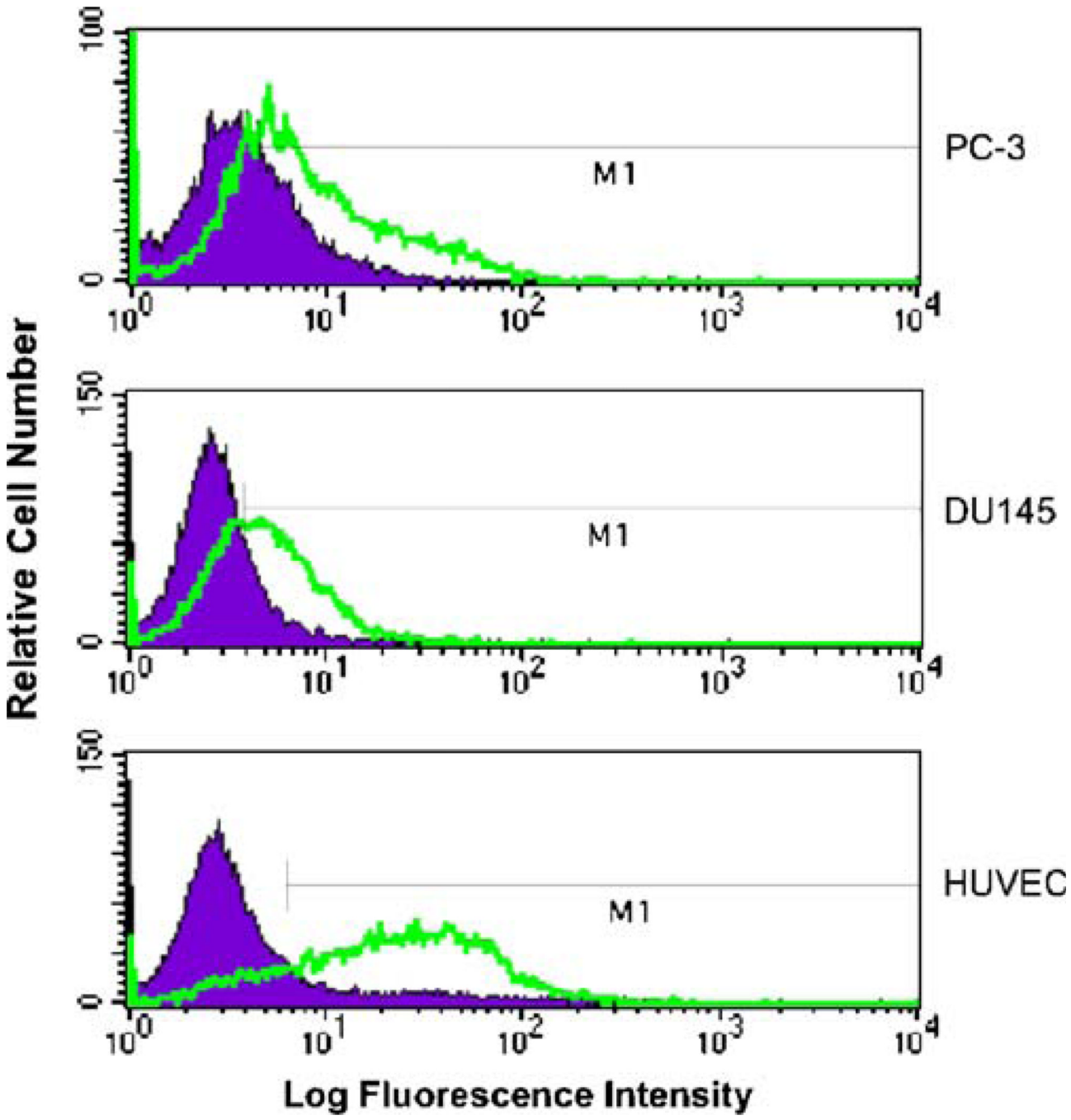

Fig. 2.

Relative expression of $\alpha_v\beta_3$ integrin. PC-3, DU145 and HUVEC cell lines were evaluated by FACS analysis following incubation with monoclonal antibody against $\alpha_v\beta_3$ and compared to control treatments.

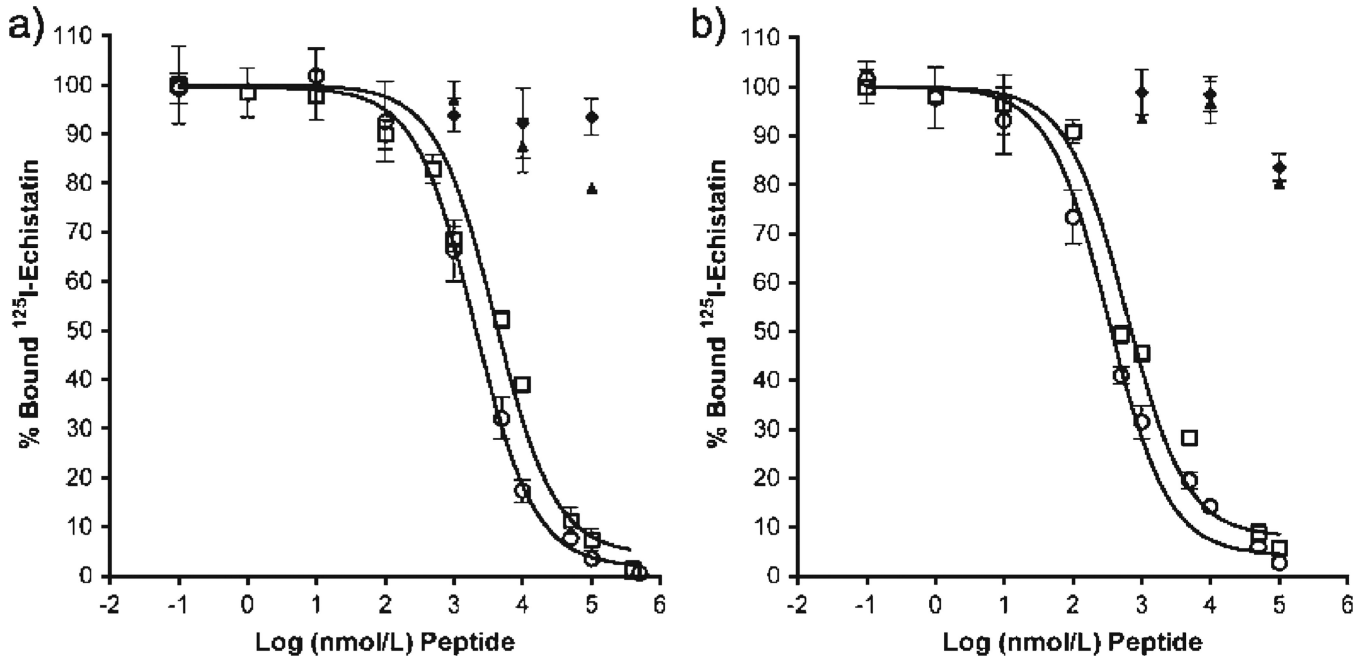

Fig. 3.

Competitive binding of HPMA copolymer conjugates and free RGDfK peptide. Competitive binding of HPMA copolymer conjugates with and without RGDfK was compared to free peptide using (**A**) PC-3 and (**B**) HUVEC cells. *Open circles* RGDfK; *open squares* P1; *closed triangles* P2; *closed diamonds* P4. Results are expressed as means of triplicate±SD.

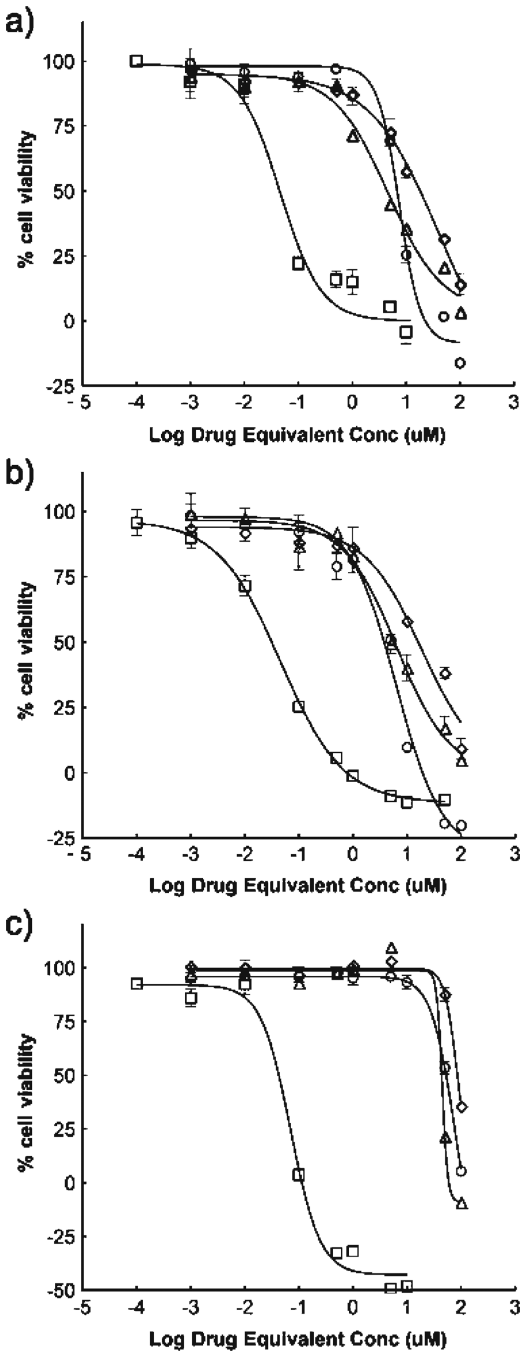

Fig. 4.

Growth inhibition effect on prostate and endothelial cell lines. (**A**) PC-3, (**B**) DU145 and (**C**) HUVEC cells treated for 72 h with drug and copolymer–drug conjugates show a loss of activity following derivatization of native GDM. Further decrease in activity not shown upon incorporation into copolymer side chains. *Squares* GDM; *triangles* AH-GDM; *circles* P1; *diamonds* P2. Results are mean±SD (*n*=4). For sample characteristics see Table I.

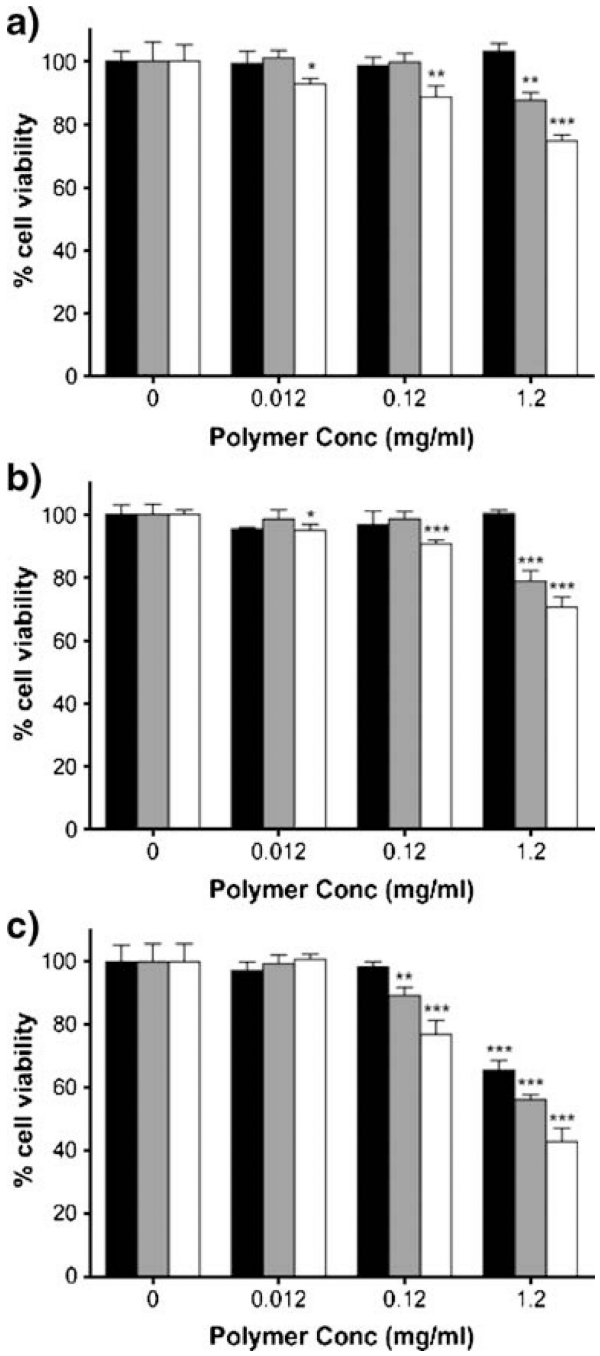

Fig. 5.

Growth inhibition effect of drug-free copolymers. (**A**) PC-3, (**B**) DU145 and (**C**) HUVEC cells treated with drug-free copolymers at polymer concentrations used in drug-containing experiments show cytotoxic effect of RGDfK-containing copolymers at high concentrations. *Black bars* P4; *gray bars* P3; *white bars* P5. Results are mean±SD (n=4). Significant differences noted as compared to untreated cells for each polymer (*$p < 0.05$; **$p < 0.01$; ***$p < 0.001$).

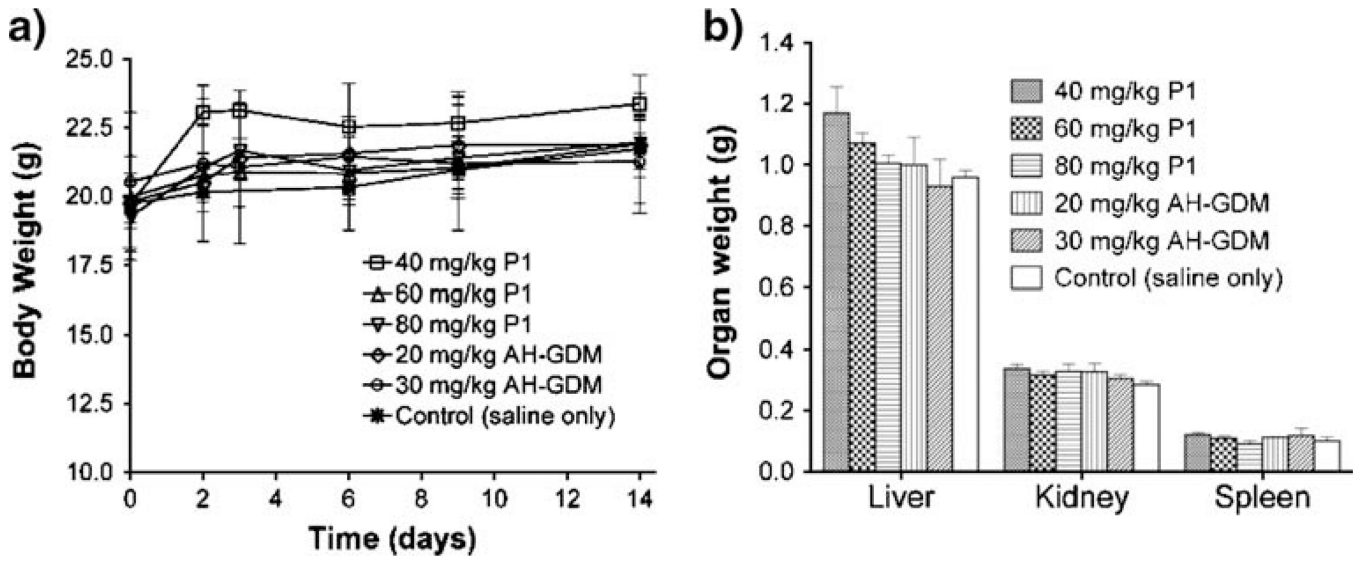

Fig. 6.

Effect of drug and polymer–drug treatments on mouse body and organ weight. Mice treated with equivalent drug dose of AH-GDM and P1 show no decrease in (**A**) body or (**B**) organ weight 14 days following a single i.v. injection. Results are expressed as means of treatment groups (*n*=3 mice)±SD. For sample characteristics see Table I.

Table I

Physicochemical Characteristics of HPMA Copolymer Conjugates Bearing AH-GDM and RGDfK

		Comonomer feed composition (mol %)						AH-GDM content[e]		RGDfK content[f]	
Polymer no.	Structure	HPMA	MA-GG-ONp	MA-GFLG-AH-GDM	MA-Tyr	Estimated M_w (kD)[b]	M_w/M_n[b,d]	mmol/g	% wt/wt	mmol/g	Peptides/ backbone[g]
1	P-(GFLG-AH-GDM)-(GG-RGDfK)	73	20	5	2	25.0[c]	1.6	0.168	10.8	0.242	6.1
2	P-(GFLG-AH-GDM)-(GG-OH)	73	20	5	2	25.0	1.6	0.168	10.8	–	–
3	P-(GFLG-OH)-(GG-RGDfK)	73	20	5[a]	2	47.0[c]	1.7	–	–	0.223	8.8
4	P-(GFLG-OH)-(GG-OH)	73	20	5[a]	2	47.0	1.7	–	–	–	–
5	P-(GG-RGDfK)	80	20	–	–	30.1[c]	1.4	–	–	0.165	6.4

[a] Reported for drug-free MA-GFLG-OH comonomer

[b] As determined by size exclusion chromatography

[c] Reported as precursor M_W

[d] Polydispersity

[e] Results of UV spectrophotometric analysis

[f] Results of amino acid analysis.

[g] Average as estimated from molecular weight and amino acid analysis data

Table II

Cathepsin B Catalyzed Drug Release from Polymer-drug Conjugates

Molecule released[a]	Polymer number	Time (min)		
		15	60	180
AH-GDM (%)	P1	6.06±0.12	11.0±0.30	15.0±0.16
	P2	7.50±0.09	15.8±0.29	22.5±0.25
Gly-AH-GDM (%)	P1	10.1±0.24	19.1±0.81	21.8±0.36
	P2	12.8±0.22	25.2±0.88	27.9±0.75
Total (%)	P1	16.2±0.36	30.1±1.10	36.9±0.50
	P2	20.3±0.32	41.0±1.15	50.4±0.92

For sample characteristics see Table I. Data represent mean ± SD (n=3)

[a] As detected by RP-HPLC

Table III

Growth Inhibition (GI_{50}) Values for Free Drug and Copolymer–Drug Conjugates in Model Cell Lines

	Cell line		
Treatment	**PC-3**	**DU145**	**HUVEC**
GDM (μM)	0.046±0.0016	0.034±0.0011	0.049±0.0012
AH-GDM (μM)	5.01±1.40	6.46±1.37	44.7±2.34
P1 (μM)	6.92±1.13	3.89±1.33	55.0±1.19
P2 (μM)	20.9±2.25	18.6±1.32	85.1±1.63

For sample characteristics see Table I

Table IV

Maximum Tolerated Dose-Finding Study in Mice Following Single Intravenous Injection

Treatment	Dose (mg/kg)[a]	N	Survivors	Day of death	Observations following injection
AH-GDM	20	3	3	–	Initial reaction to dose[b]
AH-GDM	30	3	3	–	Initial reaction to dose[b]
AH-GDM	40	2	0	1,1	Death <1 min p.i.
P1	40	3	3	–	Well tolerated[c]
P1	60	3	3	–	Well tolerated[c]
P1	80	3	3	–	Well tolerated[c]

[a] Equivalent dose of aminohexyl-geldanamycin (AH-GDM)

[b] Initial dose reaction included flush skin, decreased activity and response to touch. Normal activity resumed after 5–10 min

[c] Well tolerated dose observed by no changes in normal activity or skin color

Table V

Clinical Chemistry Parameters at Day 14 in Athymic NCr-*nu/nu* Mice Following Single i.v. Dose

Treatment	Parameter					
	ALT[a]	ALP[b]	ALB[c]	TP[d]	TBILI[e]	BUN[f]
Untreated	33.2±5.07	47.2±11.5	2.98±0.16	4.62±0.29	0.30±0.0	20.8±6.14
Saline	30.8±9.50	41.5±12.9	2.88±0.15	4.85±0.24	0.30±0.0	15.0±2.45
P1 40 mg/kg	39.3±4.16	31.3±6.66	3.03±0.15	4.93±0.23	0.33±0.1	16.7±0.58
P1 60 mg/kg	38.7±6.66	35.0±7.81	3.23±0.12	5.03±0.15	0.30±0.0	18.0±2.00
P1 80 mg/kg	37.7±2.31	37.7±10.4	3.10±0.20	4.87±0.23	0.30±0.0	15.0±1.73
AH-GDM 20 mg/kg	28.5±7.78	38.0±2.83	2.85±0.35	4.83±0.38	0.30±0.0	16.3±2.08
AH-GDM 30 mg/kg	24.7±1.53	45.7±24.4	2.63±0.25	4.70±0.26	0.67±0.6	18.0±1.00

[a] Alanine aminotransferase (u/l)

[b] Alkaline phosphatase (u/l)

[c] Albumin (g/dl)

[d] Total Protein (g/dl)

[e] Total Bilirubin (mg/dl)

[f] Blood urea nitrogen (mg/dl)